Computer Assisted Methods in Engineering and Science, **24**: 3–15, 2017.
Copyright © 2017 by Institute of Fundamental Technological Research, Polish Academy of Sciences

Biomechanical analysis of head injury caused by a charge explosion under an armored vehicle

Monika Ratajczak[1], Roman Frątczak[2], Grzegorz Sławiński[3]
Tadeusz Niezgoda[3], Romuald Będziński[1]

[1] *University of Zielona Góra*
Faculty of Mechanical Engineering
Prof. Z. Szafrana 4, 65-516 Zielona Góra, Poland
e-mail: m.ratajczak@iizp.uz.zgora.pl, r.bedzinski@ibem.uz.zgora.pl

[2] *Nobo Solutions S.A. – Nobo Solutions*
al. Kasztanowa 3a-5, 53-125 Wrocław, Poland
e-mail: roman.fratczak@nobosolutions.com

[3] *Military University of Technology*
Faculty of Mechanical Engineering
Kaliskiego 2, 00-908 Warszawa, Poland
e-mail: grzegorz.slawinski@wat.edu.pl

In this study, the authors developed the numerical model of brain structure to assess brain injury of a person in military conditions. The numerical model aimed at analyzing changes in the mechanical parameters of brain structure in the conditions of rapid overload. The results of our investigation are intended to contribute to the explanation of the phenomena of degradation of brain structures among soldiers.

Keywords: FEM, biomechanics of brain injury, combat conditions.

1. Introduction

Traumatic brain injury (TBI) is a global epidemic. The conflicts in Iraq and Afghanistan have resulted in increased numbers of veterans who have experienced TBI. The US Department of Defense and the Defense and Veterans Brain Injury Center estimate that 22% of all combat casualties from these conflicts are brain injuries. At the same time, 60% to 80% of soldiers who have other blast injuries may also have traumatic brain injuries [1]. Furthermore, in recent years the number of soldiers with the mTBI (mild traumatic brain injury) has increased significantly (Fig. 1) [2]. So many soldiers have suffered traumatic brain injuries in Iraq and Afghanistan that military medical experts have come to call it the "signature" injury of these wars [3]. It should be noted that the frequency of TBI occurrence is estimated only on the basis of the number of hospitalized cases, and the injured persons who do not request medical assistance or do not have access to medical care are not taken into consideration [4]. Another reason here is the deep-rooted tradition of soldiers hiding their physical pain and emotional turmoil for the benefit of the mission. Unfortunately, many of these brain injuries cannot be determined immediately after the accident [5]. Thus, the majority of victims live with the consequences of TBI for the rest of their lives without being aware of it. Therefore, the Centers for Disease Control and Prevention (CDC) describes TBI as America's "invisible epidemic" [2].

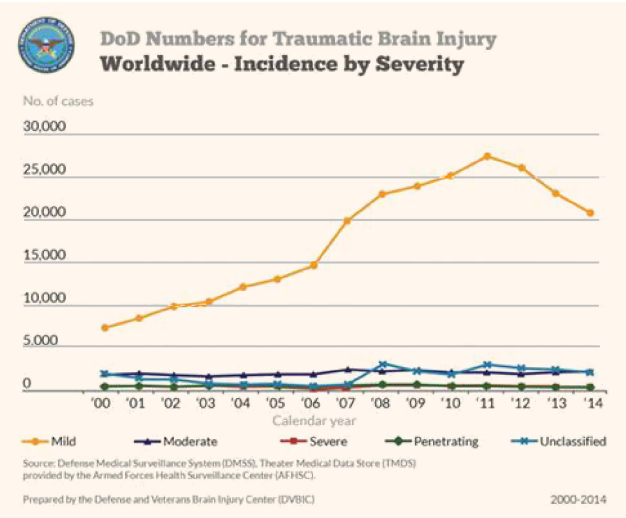

Fig. 1. Incidence of military brain injuries classified by severity, 2000–2014 [2].

From the mechanical point of view, traumatic head impact injuries occur when the human skull and brain are rapidly subjected to intolerable levels of energy. One of the causes of brain injury is relative brain motion with respect to the skull. In these traumatic events, a blow to the head or sudden acceleration/deceleration of the head without a direct impact may lead to brain lesions such as cerebral contusion, tears in arteries and veins, and tears of axons in the brain white matter. Destructive changes of brain tissues are the cause of serious neurological and neurobehavioral disorders. Depending on the injured region of the brain, soldiers may experience aphemia, aphasia, alexia, apraxia, agnosia, amnesia, ataxia, and alterations in mood or motor coordination. It is believed that neurocognitive dysfunctions result partly from excessive mechanical strains causing diffuse axonal injury (DAI), neuronal death and intracranial hematomas [6].

The major threats to soldiers taking part in contemporary military conflicts include mines and IEDs (improvised explosive devices), used mainly against armored military vehicles. Charges detonated below vehicles pose extreme danger to the crews of these vehicles [7]. In this case, brain injury can result from several external processes (Fig. 2): direct head impact with or from an object (e.g., roof and floor of the armored vehicle, another helmet, or weapons), whiplash with no direct head contact, vertical deceleration of the body (e.g., impact between the pelvis and ground), or stress force to the body remote from the head (e.g., high-pressure hit to the thorax) [8].

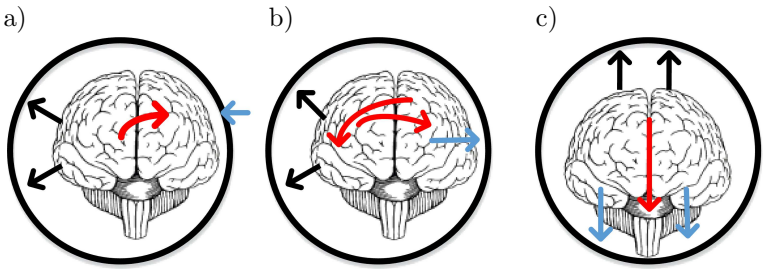

Fig. 2. Brain motions relative to the head for: a) a left side hit to the head, b) a left side hit to a vehicle (whiplash), c) a fall with the impact between the pelvis bottom and a surface. Red arrows denote brain movement at the moment of impact relative to the skull movement, black arrows in the brain denote negative pressure or tension, and blue arrows denote the initial pressure direction. Based on the Thomas F. Budinger – Editor's Note in [8].

The most common result of an explosion under the vehicle is when a human body in the vehicle is thrown by the explosion and collides with nearby objects for example, the head is hitting the

vehicle's roof (Fig. 2c and 3). Upon the charge detonation, depending on its mass and mode of initialization, the resultant mix of shock wave and shrapnel shells may cause an impulse loading to the vehicle's floor. An explosion of a mine under the vehicle's hull can cause the following: the local effect, the global effect, vehicle being thrown up in the air and the secondary effect – its drop. When it comes to the global effect, the reflected shock wave causes a displacement of the entire vehicle. The global effect occurs after 10 to 20 ms after detonation. After the vehicle reaches the maximum altitude determined, among others, by its mass and the exploding charge dimensions, it begins to fall down after 100 to 300 ms [9] (Fig. 3).

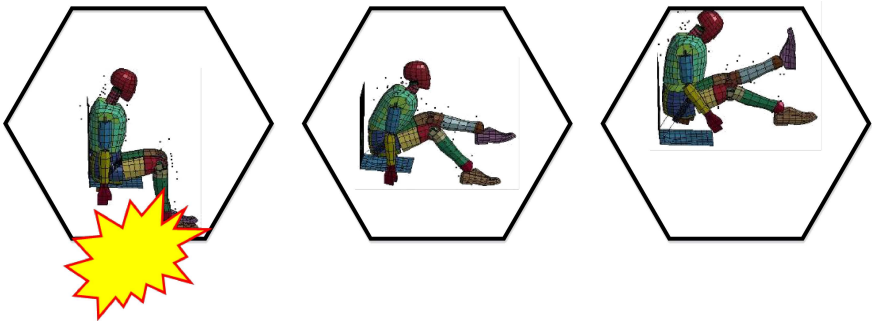

Fig. 3. The impact of an explosion on a crew of armored vehicle.

As a result of the head impact with the vehicle roof, the brain undergoes displacement relative to the skull and the bridging veins undergo the process of shearing, which leads to the development of subdural hematoma. The biomechanical responses, in the form of internal stresses and strains, could be responsible for TBIs. In a biomechanical analysis of the head under an impact force the important brain injury criteria are intracranial pressures, strain, and stress.

A number of studies have pointed out that brain deformation or strain is a principal cause of brain injury. Unfortunately, measuring the brain strain resulting from accelerations, especially *in vivo*, is practically impossible during an impact [10, 11]. At the same time the physical models require selection of mechanical properties of materials, which poses a considerable problem since biological tissues are involved. Therefore, at present one of the most effective ways of identifying the response of brain structures to loading is numerical modelling [12]. In particular, the finite element method designed for models of irregular geometry, composite materials and complex loading as well as complex boundary conditions is now the preferred method for studying head injuries The development of head numerical models allows a better understanding of damage mechanisms, response and tolerance levels.

Despite the recent efforts in the development of finite element (FE) human head models, a model capable of capturing head responses by taking into account the cerebrovascular system during a charge explosion under military vehicles has not been reported. In this work a new FE brain tissue model is proposed to evaluate the extent of brain tissue injury as a result of an explosion under a military vehicle. In our study, we analyzed the displacement of passengers' heads due to explosion under the armored vehicle. The main objective of the current study was to evaluate the strains and stress in the main regions of the brain as predictors of damage and determine the associations between brain tissue deformations and injury.

2. Method and materials

2.1. Load conditions

In this study, we analyzed the impact of sudden load on the passenger in the vehicle due to an explosion under the right frontal wheel. The boundary conditions were taken from previous

numerical studies presented in [13]. The values used in this part were read from the sensors placed on the head and neck of the anthropometric hybrid III dummy, which was located in the armored transporter during the explosion. We analyzed the critical case when a soldier hit his head on the roof of the vehicle. We analyzed both the responses of the passenger with seat belt and without seat belt (Fig. 4).

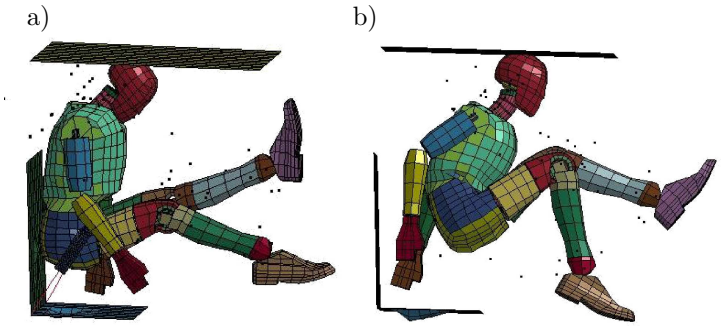

Fig. 4. The passenger: a) with seat belt and b) without seat belt.

2.2. Head FE model

The geometry of the human tissue was obtained using medical images with a very thick mesh sampling. Next, the medical images were segmented using a medical imaging tool in which a simplified 3D geometry of the skull and the brain was formed. Subsequently, the model was imported into the LS-DYNA program, where additional geometry of the brain structure was constructed. The head model includes the skull, brain, cerebellum, meninges (dura mater and pia mater) cerebrospinal fluid (CSF), sinus sagittalis superior (SSS), falx cerebri, tentorium cerebelli and bridging veins (Figs. 5–7).

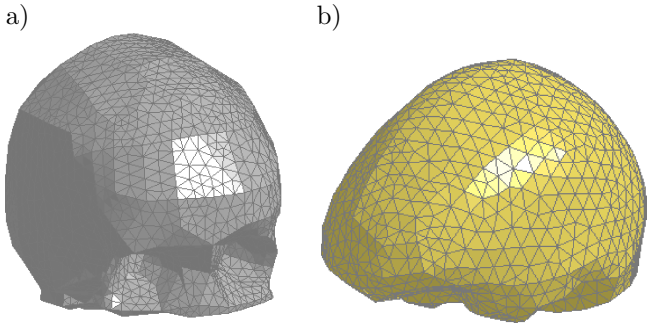

Fig. 5. FE head model: a) skull, b) brain.

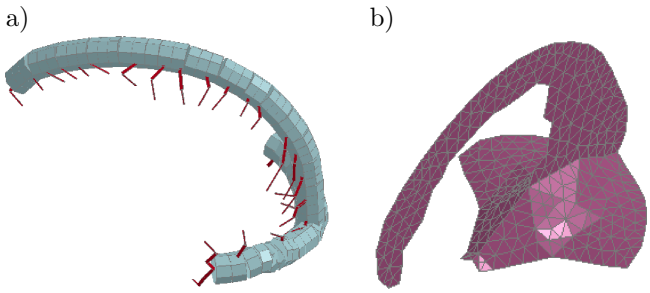

Fig. 6. FE head model: a) bridging veins and sinus sagittalis superior, b) falx cerebri and tentorium cerebelli.

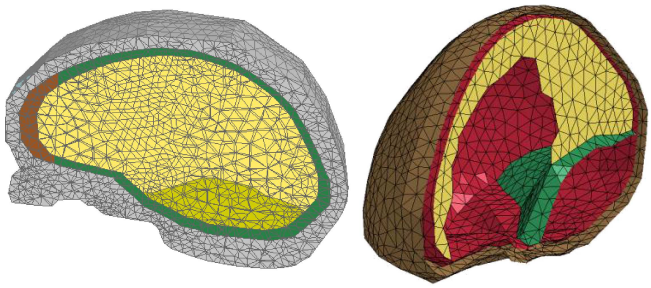

Fig. 7. The cross-section of the head FE model.

This model does not include the skin and neck muscles because they do not contribute to the response of the brain tissue controlled by kinematic extortion. The bridging veins were divided into the frontal, parietal and occipital regions. All simulations were conducted with LS-Dyna using an explicit dynamic solving method. The head model consisted of 55 118 solid elements, 6238 shell elements, and 151 beam elements. The element types and the corresponding FE numbers for each anatomical component can be found in Table 1.

Table 1. Element type and number of corresponding FEs of the brain structure.

Brain structure	Element type and number of finite elements		
	Solid	Shell	Beam
Skull	27 577	–	–
Dura mater	–	3158	–
Pia Mater	–	2454	-
Cerebrum	15 333	–	–
Cerebellum	2508	–	–
CSF	9700	–	–
SSS and BV			151
Falx cerebri	–	270	–
Tentorium cerebelli	–	356	–

The numerical model consisted of heterogeneous multiphase materials. The results obtained by Fahlsted et al. [14] and his rationale for the modelling of skull bones were used. The Young modulus was assumed to be 15 000 MPa, the Poisson ratio is 0.22 and density is 2000 kg/m^3. The mechanical values for dura mater were taken as in Kleiven [15] and Brands et al. [16], where the Young modulus is 31.5 MPa, the Poisson ratio is 0.45 and density is 1130 kg/m^3. The mechanical properties of falx cerebri and tentorium cerebelli were modelled in the work of Kleiven [15]. Mechanical parameters of bridging veins in the frontal, parietal and occipital regions were estimated on the basis of mechanical characteristics obtained in experimental studies on human samples made post-mortem and taken from patients in whose cases a mechanical head injury was excluded [17]. Exemplary characteristics of stress and strain for a bridging vein are presented in Fig. 8.

The brain tissue was modelled taking into account the viscoelastic properties with shear relaxation behavior described by:

$$G(t) = G_\infty + (G - G_\infty) \cdot e^{-\beta t}, \tag{1}$$

where G_∞ – long-time (infinite) shear modulus, G – short-time shear modulus, β – decay coefficient, t – time.

The solid materials used in this work were based on the research conducted by D. Baumgartner and G. Belingardi. The mechanical properties of all the components of the head FE model are summarized in Table 2.

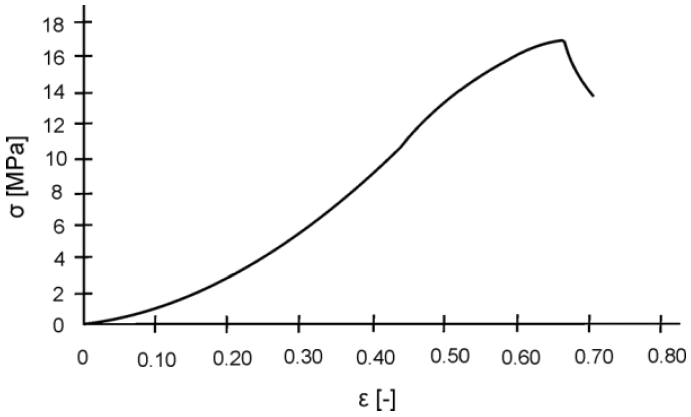

Fig. 8. Characteristics of stress [MPa] – strain [–] of the bridging veins [17].

Table 2. Mechanical properties of the head structure.

Element	Young's modulus [MPa]	Density [kg/m^3]	Poisson's ratio
Skull	15 000	2000	0.22
Dura mater	31.5	1130	0.45
Pia Mater	30	1130	0.45
CSF**	K^* = 2200 MPa	1000	0.49
SSS	28.2	1040	0.45
Falx cerebri and Tentorium cerebelli	31.5	1130	0.45
Cerebrum and Cerebellum	K^* = 1125 MPa G = 0.49 MPa G_∞ = 0.0167 MPa β = 0.145 ms^{-1}	Viscoelastic model	

$^*K$ – Bulk modulus, ** model – FLUID_ELASTIC_FLUID

3. Results

As a result of the numerical analysis, the critical values of strain, stress and displacement for the numerical components were obtained (Figs. 9–20).

- Results for the passenger with seat belt (Figs. 9–14):

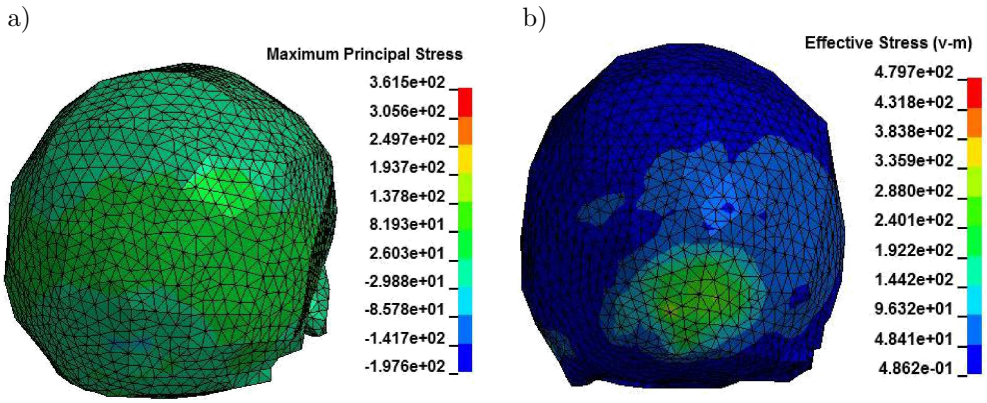

Fig. 9. a) Maximum principal stress on the skull, b)von Mises stress.

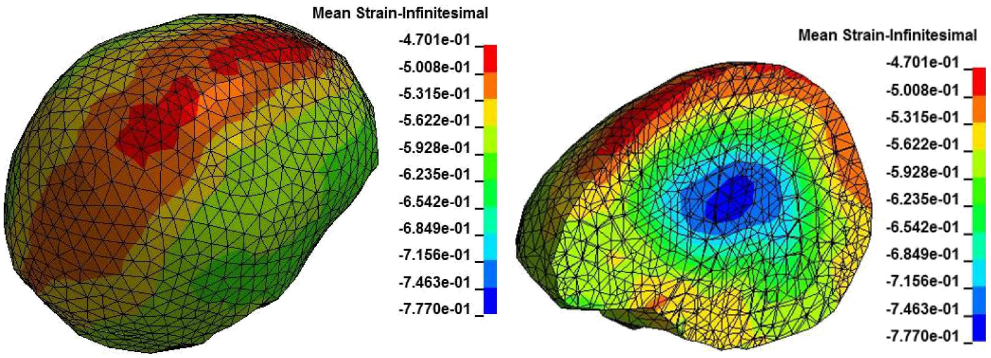

Fig. 10. Strain distribution on the brain.

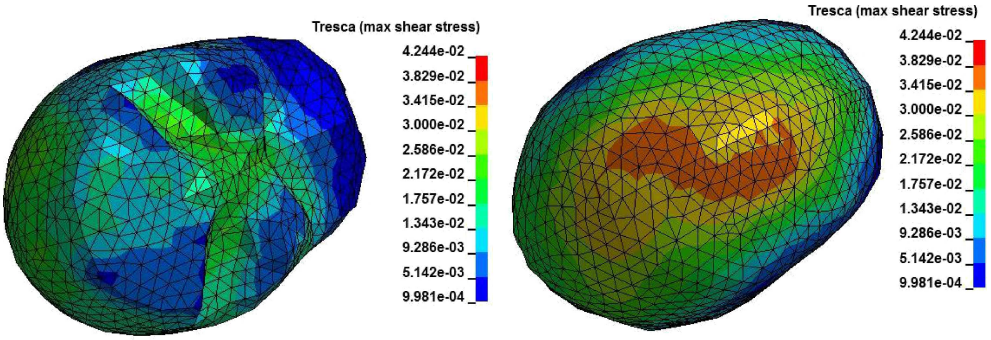

Fig. 11. Shear stress in the brain.

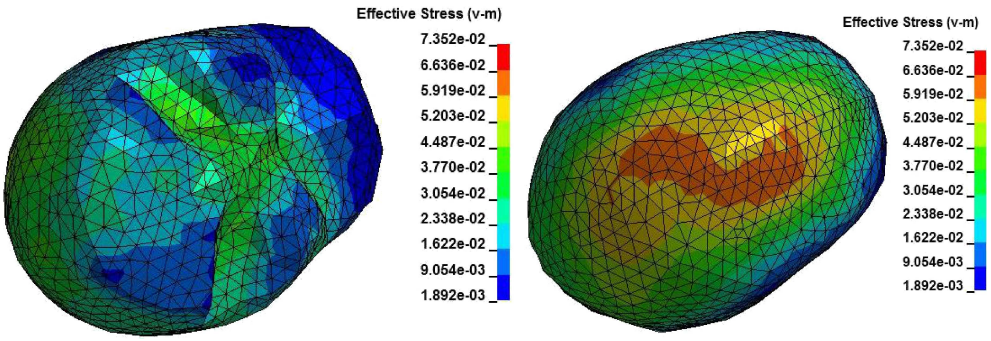

Fig. 12. The von Mises stress on the brain.

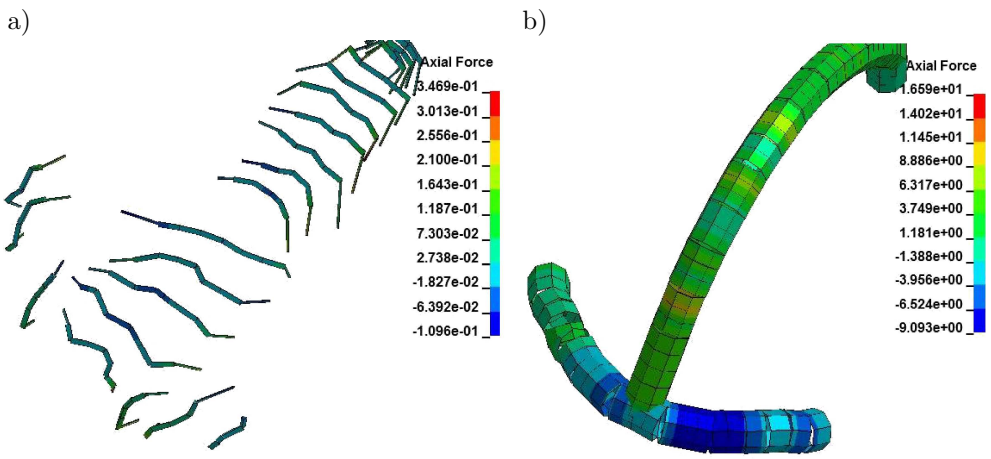

Fig. 13. a) Axial force in the bridging vein, b) axial force on the superior sagittal sinus.

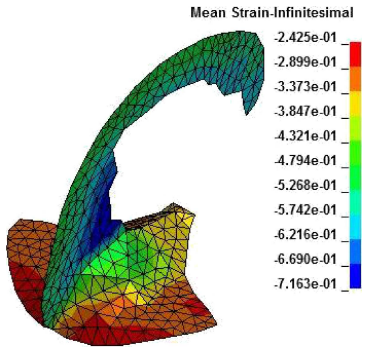

Fig. 14. Strain distribution for falx cerebri and tentorium cerebelli.

- Results for the passenger without seat belt (Figs. 15–20):

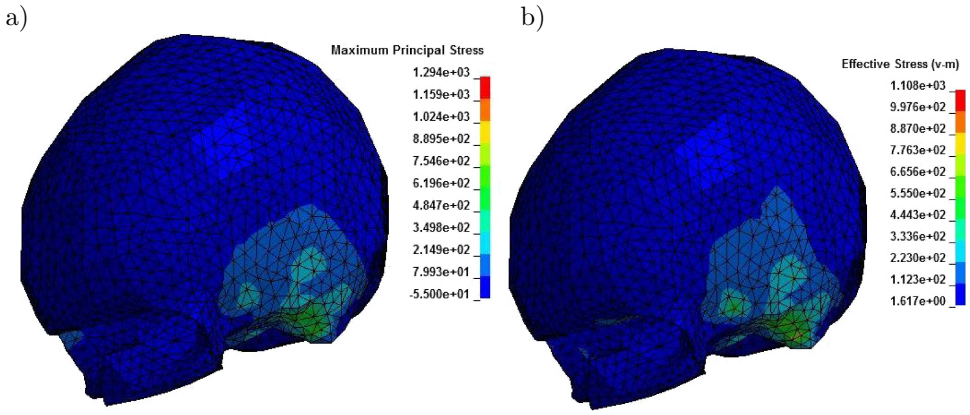

Fig. 15. a) Maximum principal stress on the skull, b) the von Mises stress.

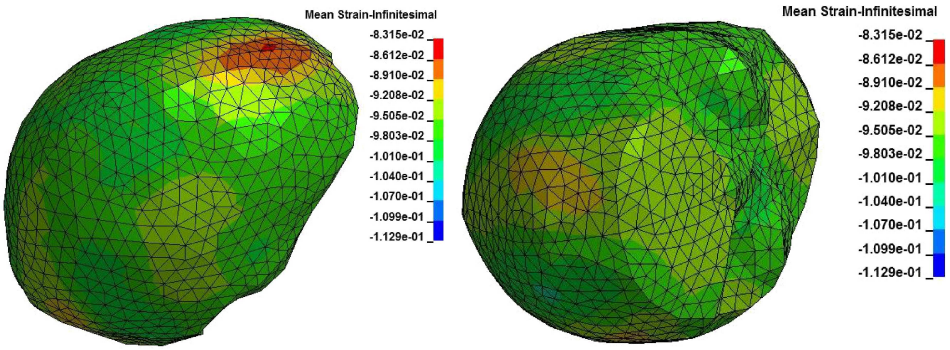

Fig. 16. Strain distribution on the brain.

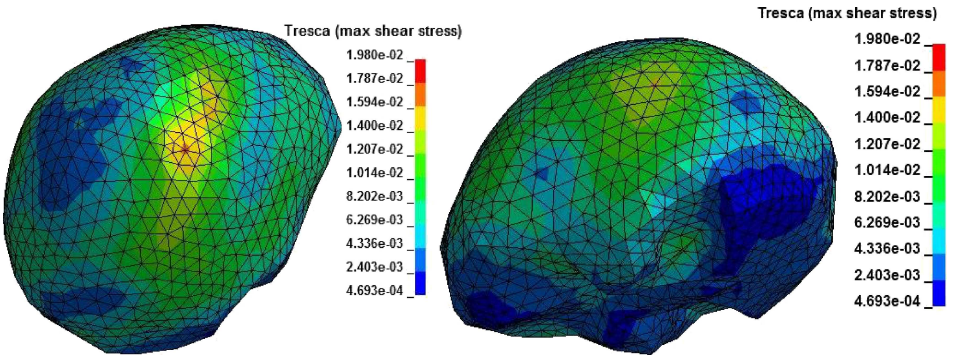

Fig. 17. Shear stress in the brain.

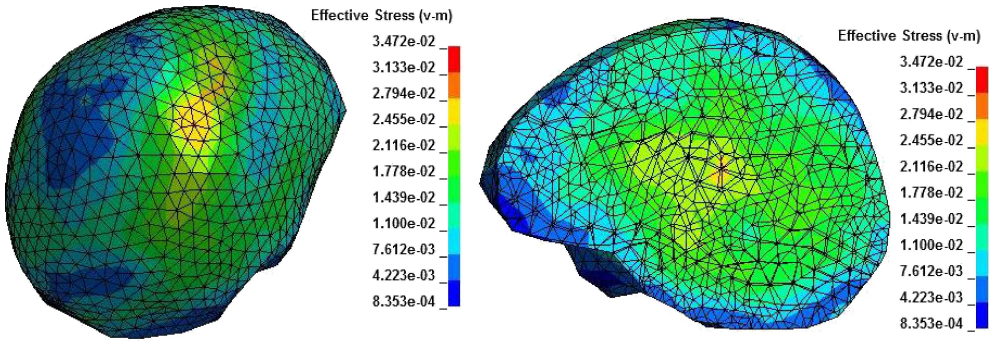

Fig. 18. The von Mises stress on the brain.

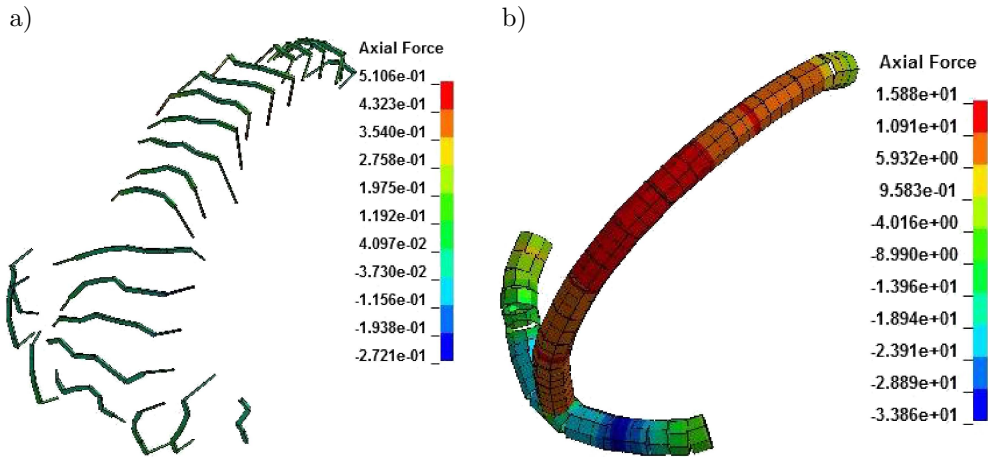

Fig. 19. a) Axial force in the bridging vein, b) axial force on the superior sagittal sinus.

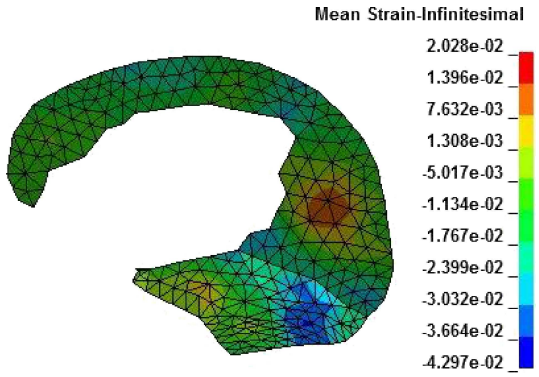

Fig. 20. Strain distribution for falx cerebri and tentorium cerebelli.

The maximum values of each component are summarized in Tables 3–5.

Table 3. Maximum values for the skull.

Maximum values	Passenger without seat belt	Passenger with seat belt
Strain	0.08	0.47
Shear stress	19 kPa	42 kPa
Von Mises stress	34 kPa	73 kPa

Table 4. Maximum values for the brain.

Maximum values	Passenger without seat belt	Passenger with seat belt
Principal stress	1294 MPa	361 MPa
von Mises stress	1108 MPa	479 MPa

Table 5. Maximum values for the other components of the brain.

Maximum values	Passenger without seat belt	Passenger with seat belt
Bridging veins (BV) (axial force)	0.5 N	0.3 N
Superior Sagittal Sinus (SSS) (axial force)	15.88 N	16.59 N
Falx cerebri and tentorium cerebelli (strain)	0.02	0.24

Based on our numerical analysis and the experimental research described in the literature (Tables 6–10), we conducted an assessment of brain tissue destruction. In both passengers (with and without seat belt) we noticed a fracture of the skull (Figs. 9 and 15). Even though the obtained values of stress on the skull were higher in the case of a passenger without a seat belt, a greater destruction of brain tissue, including neurological dysfunctions, was observed in the passenger wearing a seat belt (Figs. 16–18). The analysis of strains shows that in the passenger with seat belt a structural failure occurs and the probability of the occurrence of mild TBI in the brain is 80% (Table 7). On the basis of the analysis of shear stress (Table 9) and von Mises stress (Table 8) we found that the passenger with seat belt suffered from concussion and moderate neurological lesions. However, in case of the passenger wearing seat belt the probability of severe neurological lesions and axonal damage was 50%. Furthermore, in the same passenger we observed a diffuse axonal injury in the midbrain region. Rapid movements of various parts of the brain and cerebellum resulted in the compression of the falx cerebri and tentorium cerebelli (Figs. 14 and 20). Another important factor in intracranial injuries is rupture of the bridging veins. The large displacement of the brain relative to the skull caused the interruption of the bridging veins and formation of subdural hematoma.

Table 6. Various proposals for thresholds of skull criteria in the literature.

Reference	von Mises stress
McElhaney et al. [18]	34.47–103.42 MPa – Skull fracture
Schaller et al. [19]	153 MPa – Skull fracture

Table 7. Various proposals for thresholds of brain structure criteria in the literature.

Reference	Strain
Galbraith et al. [20]	> 0.25 – Structural failure > 0.20 – Functional deficit < 0.10 – Reversible injury
Shreiber et al. [21]	> 0.188 Blood-brain barrier injury
Bain and Meaney [22]	> 0.13 – 25% probability of mild TBI (conservative) > 0.18 – 50% probability of mild TBI (optimal) > 0.28 – 80% probability of mild TBI (liberal)
Zhang et al. [23]	> 0.14 – 25% probability of mild TBI (conservative) > 0.19 – 50% probability of mild TBI (optimal) > 0.24 – 80% probability of mild TBI (liberal)
Deck and Willinger [24]	≥ 0.18 – Axonal damage

Table 8. Various proposals for thresholds of brain structure criteria in the literature.

Reference	von Mises stress
Zhou et al. [25]	≥ 11 kPa – Brain injury (in car accident)
Kang et al. [26]	≥ 15 kPa – Brain injury (in motorcycle accident)
Miller et al. [27]	> 7 or 8.6 kPa – Contusion
Anderson et al. [28]	≥ 27 kPa – Brain injury (live animal testing)
Newman [29]	≥ 20 kPa – Mild traumatic brain injuries (TBIs)
Willinger and Baumgartner [30]	15–20 kPa – Injury (concussion)
Baumgartner et al. [31]	> 27 kPa – 50% probability of moderate neurological injury > 39 kPa – 50% probability of severe neurological
Baumgartner and Willinger [32]	> 18 kPa – 50% probability of moderate neurological lesions > 38 kPa – 50% probability of severe neurological lesions
Deck and Willinger [24]	≥ 26 kPa – Axonal damage

Table 9. Various proposals for thresholds of brain structure injury criteria in the literature.

Reference	Region	Shear stress
Claessens et al. [26]	Midbrain	11–16.5 kPa – Severe Injury
Anderson et al. [33]	Midbrain	8–16 kPa – Severe Injury (mild diffuse axonal injury or DAI)
Zhang et al. [23]	Midbrain	6.2–10.6 kPa – Injury 3.4–7.2 kPa – Non-injury
Zhang et al. [23]	Midbrain	> 6.6 kPa – Injury
Zhang et al. [23]	Upper brainstem	> 7.8 kPa – 50% probablility of mild TBI (optimal)
Zhang et al. [23]	Thalamus	3.3–5.7 kPa – Injury

Table 10. The maximum force tearing the bridging veins in various regions of the head [17].

Mechanical properties of the bridging veins	Frontal region	Parietal region	Occipital region
$F_{\max}$ [N]	0.43	0.53	0.64

A numerical analysis of the distribution of the maximum forces acting on the vessel was carried out (Figs. 13 and 19). Based on the limit values [17] (Table 10), it was found that the bridging veins and superior sagittal sinus in the frontal and occipital region were damaged in the passenger without a seat belt.

4. Conclusions

The presented study focused on the analysis of changes in the mechanical parameters of the brain structure that have been affected by heavy impact loading. We analyzed the effect of mechanical forces on the brain tissue of passengers in the vehicle. The numerical results were compared with the experimental studies described in the literature and this allowed us to provide the neurological assessment. Head injury is a result of a series of mechanical interactions. This study provides new insights into brain injuries among soldiers. The initial state (position) of a soldier is an important factor influencing the obtained results. We concluded that the use of seat belt changed the trajectory of head movement causing a larger displacement in the horizontal direction. At the same time, the use of seat belt eliminates the risk of the head contact with the vehicle roof, as it is shown in the distributions of stresses on the skull. In both cases the skull was fractured. Despite the fact

that the stress values on the skull were three times higher for the passenger without a seat belt, greater neurological damage occurred in the passenger wearing a seat belt. This is due to a rapid displacement of the brain weight relative to the skull as a result of a sudden jerk. It is interesting that damage to the bridging veins was observed in the passenger without a seat belt. Analyzing the distributions of axial forces on the bridging veins and superior sagittal sinus we found that the damage occurred in the outflow cuff segment (point connection of BV with SSS). This fact is consistent with the literature because damage occurs most frequently in this region [34]. Gradually, high shear stresses are concentrated at the white matter and corpus callosum. As expected, with an increase of the shockwave, the maximum averaged shear strains will increase and decrease, respectively. Mechanically induced brain deformation at a particular region, or site, as a consequence of applied loading, may determine a particular type of brain injury. Outcomes from our model can be employed to establish a relationship between the severity and scope of the functional, or structural, failures and the extent of the input impact loads. The conducted numerical analysis, combined with widespread experimental studies can be of utmost significance in the assessment of stroke and impact loading effects among soldiers taking part in combat operations.

Acknowledgement

This research work was carried out under the project DOBR-BIO/22/13149/2013: "Safety improvement and protection of soldiers on missions through operation in military – medical and technical areas" sponsored by the National Centre for Research and Development in Poland, Military University of Technology, Warsaw, Poland.

References

[1] E. Lanier Summerall. Report of (VA) Consensus Conference: Practice Recommendations for Treatment of Veterans with Comorbid TBI, Pain, and PTSD. 17 pages, 2010.

[2] http://dvbic.dcoe.mil/dod-worldwide-numbers-tbi.

[3] Independent Review Group. *Report on Rebuilding the Trust: Rehabilitative Care and Administrative Processes at Walter Reed Army Medical Center and National Naval Medical Center*. 129 pages, April 2007. http://www.nvti.ucdenver.edu/resources/VETSNET/vol15no2/IRG-Report-Final.pdf.

[4] T.W. McAllister. Neurobehavioral sequelae of traumatic brain injury: evaluation and management. *World Psychiatry: Official Journal of the World Psychiatric Association (WPA)*, **7**: 3–10, 2008. http://www.pubmedcentral.nih.gov/articlerender.fcgi?artid=2327235&tool=pmcentrez&rendertype=abstract.

[5] A.D. Gean. *Brain Injury: Applications from War and Terrorism*. Wolters Kluwer Health/Lippincott Williams & Wilkins, USA, 2014. https://books.google.com/books?id=nmAGBAAAQBAJ&pgis=1.

[6] E. Wiczkowski, A. Kędzia, A. Kania. Traumatic damage pathomechanism of cerebral vessels caused by geriatric changes. *Engineering Transactions*, **51**(2–3): 339–347, 2003.

[7] T. Klekiel. Biomechanical analysis of lower limb of soldiers in vehicle under high dynamic load from blast event. *Series on Biomechanics*, **29**(2-3): 14–30, 2015. http://www.imbm.bas.bg/biomechanics/uploads/Archive2015-2-3/14-30.pdf.

[8] National Academy of Engineering. Concussion: A National Challenge. *The Bridge*, **46**, 132 pages, Washington, DC, 2016.

[9] E. Krzystała, A. Mężyk, S. Kciuk. Analysis of threat to crew posed by explosion of charge placed under wheeled armoured vehicle [in Polish]. *The Journal of Science of the Gen. Tadeusz Kosciuszko Military Academy of Land Forces*, **1**(159): 145–154, 2011.

[10] K. Miller [Ed.]. *Biomechanics of the Brain*. Springer Science & Business Media, 2011. https://books.google.com/books?id=XwS3lOWQXxEC&pgis=1.

[11] P.J. Prendergast. An analysis of theories in biomechanics. *Engineering Transactions*, **49**(2-3): 117–133, 2001.

[12] M. Ratajczak, M. Sąsiadek, R. Będziński. An analysis of the effect of impact loading on the destruction of vascular structures in the brain. *Acta of Bioengineering and Biomechanics*, **18**, 2016. doi:10.5277/ABB-00552-2016-02.

[13] G. Sławiński, T. Niezgoda, W. Barnat, M. Wojtkowski. Numerical analysis of the influence of blast wave on human body, *Journal of KONES Powertrain and Transport*, **20**(3): 381–386, 2013.

[14] M. Fahlstedt, K. Baeck, P. Halldin, J. Vander Sloten, J. Goffin, B. Depreitere, S. Kleiven. Influence of impact velocity and angle in a detailed reconstruction of a bicycle accident. *Proceedings of the International Research Council on the Biomechanics of Injury Conference*, **40**: 787–799, 2012.

[15] S. Kleiven. Predictors for traumatic brain injuries evaluated through accident reconstructions. *Stapp Car Crash Journal*, **51**: 81–114, 2007. http://www.ncbi.nlm.nih.gov/pubmed/18278592.

[16] D.W.A. Brands, P.H.M. Bovendeerd, J.S.H.M. Wismans. On the potential importance of non-linear viscoelastic material modelling for numerical prediction of brain tissue response: test and application. *Stapp Car Crash Journal*, **46**: 103–121, 2002. http://www.ncbi.nlm.nih.gov/pubmed/17096221.

[17] M. Horanin-Dusza. *The analysis of the biomechanical and histological properties of cerebral bridging veins in alcoholics and nonalcoholics – the importance in the subdural hematomas etiology* [in Polish]. PhD Thesis, Medical University, Wrocław, Poland, 2009.

[18] J.H. McElhaney, P.I. Mate, V.L. Roberts. A new crash test device – "Repeatable Pete". *Proceedings of 17th Stapp Car Crash Conference*, 1973. doi:10.4271/730983.

[19] A. Schaller, C. Voigt, H. Huempfner-Hierl, A. Hemprich, T. Hierl. Transient finite element analysis of a traumatic fracture of the zygomatic bone caused by a head collision. *International Journal of Oral and Maxillofacial Surgery*, **41**(1): 66–73, 2012. doi:10.1016/j.ijom.2011.09.004.

[20] J.A. Galbraith, L.E. Thibault, D.R. Matteson. Mechanical and electrical responses of the squid giant axon to simple elongation. *Journal of Biomechanical Engineering*, **115**: 13–22, 1993. http://www.ncbi.nlm.nih.gov/pubmed/8445893.

[21] D.I. Shreiber, A.C. Bain, D.F. Meaney. In vivo thresholds for mechanical injury to the blood-brain barrier. *Proceedings of 41st Stapp Car Crash Conference*, 1997.

[22] A.C. Bain, D.F. Meaney. Tissue-level thresholds for axonal damage in an experimental model of central nervous system white matter injury. *Journal of Biomechanical Engineering*, **122**(6): 615–622, 2000. http://www.ncbi.nlm.nih.gov/pubmed/11192383.

[23] L. Zhang, K.H. Yang, A.I. King. A proposed injury threshold for mild traumatic brain injury. *Journal of Biomechanical Engineering*, **126**(2): 226–236, 2004. http://www.ncbi.nlm.nih.gov/pubmed/15179853.

[24] C. Deck, R. Willinger. Improved head injury criteria based on head FE model. *International Journal of Crashworthiness*, **13**(6): 667–678, 2008. http://dx.doi.org/10.1080/13588260802411523.

[25] C. Zhou, T.B. Khalil, A.I. King. A new model comparing impact responses of the homogeneous and inhomogeneous human brain. SAE Technical Paper 952714. *Proceedings of 39th Stapp Car Crash Conference*, 1995. doi:10.4271/952714.

[26] M. Claessens, F. Sauren, J. Wismans. Modeling of the human head under impact conditions: A parametric study. *Proceedings of 41st Stapp Car Crash Conference*, 1997. doi:10.4271/973338.

[27] R.T. Miller, S.S. Margulies, M. Leoni, M. Nonaka, X. Chen, D.H. Smith. Finite element modeling approaches for predicting injury in an experimental model of severe diffuse axonal injury. *SAE Technical Paper 983154*, 1998. doi:10.4271/983154.

[28] D.W. Anderson, W.D. Kalsbeek, T.D. Hartwell. The national head and spinal cord injury survey. *Journal of Neurosurgery*, **53**, Suppl: S19–31, 1980.

[29] J.A. Newman. A generalized acceleration model for brain injury threshold (GAMBIT). *Proceedings of International Conference on the Biomechanics of Impact*, pp. 121–131, 1986.

[30] R. Willinger, D. Baumgartner. Human head tolerance limits to specific injury mechanisms. *International Journal of Crashworthiness*, **8**(6): 605–617, 2003. doi:10.1533/ijcr.2003.0264.

[31] D. Baumgartner, R. Willinger, N. Shewchenko, M.C. Beusenberg. Tolerance limits for mild traumatic brain injury derived from numerical head impact replication. *Proceedings of the International Conference on the Biomechanics of Impacts (IRCOBI)*, Isle of Man, **29**: 353–355, 2001.

[32] D. Baumgartner, R. Willinger. Numerical modeling of the human head under impact: new injury mechanisms and tolerance limits. In: *IUTAM Symposium on Impact Biomechanics: From Fundamental Insights to Applications*, M.D. Gilchrist [Ed.]. Springer, pp. 195–203, 2005. doi:10.1007/1-4020-3796-1_20.

[33] R.W.G. Anderson, C.J. Brown, P.C. Blumbergs, G. Scott, J.W. Finney, N.R. Jones, A.J. McLean. Mechanisms of axonal injury: an experimental and numerical study of a sheep model of head impact. *Proceedings of the International Conference on the Biomechanics of Impact (IRCOBI*), Sitges, Spain, pp. 107–120, 1999.

[34] N. Famaey, Z. Ying Cui, G. Umuhire Musigazi, J. Ivens, B. Depreitere, E. Verbeken, J.V. Sloten. Structural and mechanical characterisation of bridging veins: A review. *Journal of the Mechanical Behavior of Biomedical Materials*, **41**: 222–240, 2015. doi:10.1016/j.jmbbm.2014.06.009.